A mouse p53 mutant lacking the proline-rich domain rescues Mdm4 deficiency and provides insight into the Mdm2-Mdm4-p53 regulatory network

Franck Toledo,[1,2,*] Kurt A. Krummel,[1] Crystal J. Lee,[1] Chung-Wen Liu,[1] Luo-Wei Rodewald,[1] Mengjia Tang,[1] and Geoffrey M. Wahl[1,*]

[1] The Salk Institute for Biological Studies, Gene Expression Laboratory, 10010 North Torrey Pines Road, La Jolla, California 92037
[2] Institut Pasteur, Unité d'Expression Génétique et Maladies, FRE CNRS 2850, 25 Rue du Docteur Roux, 75724 Paris, Cedex 15, France
*Correspondence: ftoledo@pasteur.fr (F.T.); wahl@salk.edu (G.M.W.)

Summary

The mechanisms by which Mdm2 and Mdm4 (MdmX) regulate p53 remain controversial. We generated a mouse encoding p53 lacking the proline-rich domain ($p53^{\Delta P}$). $p53^{\Delta P}$ exhibited increased sensitivity to Mdm2-dependent degradation and decreased transactivation capacity, correlating with deficient cell cycle arrest and reduced apoptotic responses. $p53^{\Delta P}$ induced lethality in $Mdm2^{-/-}$ embryos, but not in $Mdm4^{-/-}$ embryos. Mdm4 loss did not alter Mdm2 stability but significantly increased $p53^{\Delta P}$ transactivation to partially restore cycle control. In contrast, decreasing Mdm2 levels increased $p53^{\Delta P}$ levels without altering $p53^{\Delta P}$ transactivation. Thus, Mdm4 regulates p53 activity, while Mdm2 mainly controls p53 stability. Furthermore, Mdm4 loss dramatically improved $p53^{\Delta P}$-mediated suppression of oncogene-induced tumors, emphasizing the importance of targeting Mdm4 in chemotherapies designed to activate p53.

Introduction

Stringent regulation of p53 in response to stress is essential to suppress tumor formation. p53 is a transcription factor maintained at low levels under normal conditions. Upon stress, it is stabilized and activated to induce the transcription of genes involved in cell cycle arrest, apoptosis, and DNA repair (Wahl et al., 2005, for review). Nontranscriptional mechanisms for apoptosis induction have also been proposed (Chipuk et al., 2004). A complex interplay of numerous proteins regulates p53. For example, the interaction of the histone acetyl transferase p300 with the p53 N-terminal transactivation domain (TAD) is important for efficient transactivation, but the same TAD is inhibited by interaction with Mdm2 and its related family member Mdm4 (also called MdmX) (Marine and Jochemsen, 2005). The stability of p53 is regulated primarily by the E3 ubiquitin-ligase activity of Mdm2, with possible additional contributions from other ubiquitin ligases (Pirh2, COP1, Birc6), the ubiquitin-specific protease HAUSP, and other modulators such as ARF, Pin1, or YY1 (Brooks and Gu, 2004; Mantovani et al., 2004; Ren et al., 2005; Sui et al., 2004). The importance of this pathway in tumor suppression is indicated by p53 mutations in >50% of human cancers, and Mdm2 or Mdm4 overexpression in many of the remainder (Danovi et al., 2004; Vassilev et al., 2004; Vousden and Lu, 2002).

The contribution of p53 structure to target gene regulation remains to be resolved. For example, the proline-rich domain (PRD), defined by residues 58–98 of human p53, contains 15 prolines and five repeats of the amino acid motif PXXP (where P designates proline and X any amino acid; Figure 1A). PXXP motifs can create binding sites for SH3 (Src homology 3) domains, and the p53 PXXPs appear to affect interaction with the histone acetyl transferase p300 (Dornan et al., 2003). The PRD also may modulate Mdm2-mediated degradation, since the conformation of prolines in the PRD can be changed upon binding of the prolyl isomerase Pin1 after stress to reduce Mdm2 binding (Mantovani et al., 2004). These and other data implicate the PRD in p53 stability control, p53-mediated transactivation, and transcription-independent apoptosis (Berger et al., 2001; Chipuk et al., 2004; Dumaz et al., 2001; Edwards et al., 2003). However, transfection studies have produced conflicting data concerning the contribution of the PRD to p53 functional output. Walker and Levine (1996) showed that a human p53 lacking residues 62–91 ($p53^{\Delta P}$) was stabilized after stress but compromised for growth suppression (Figure 1A). Later studies reported that $p53^{\Delta P}$ is able to induce cell cycle arrest

SIGNIFICANCE

This work presents a p53 mutant protein able to rescue lethality caused by Mdm4 deficiency. This unique property allowed us to test the effects of Mdm4 loss on Mdm2 and p53 stability, and p53 transactivation and function in vivo. Our results are not consistent with previous models of p53 regulation by Mdm2 and Mdm4, but rather suggest an alternative regulation model. Furthermore, chemotherapeutic strategies designed to activate p53 in tumors have so far focused on interfering with Mdm2. Our finding that Mdm4 deficiency improves the capacity of a mutant p53 to suppress oncogene-induced tumors offers genetic evidence that additional strategies should be designed to abrogate p53-Mdm4 interactions. Our results suggest that Mdm2 and Mdm4 antagonists could cooperate to activate p53.

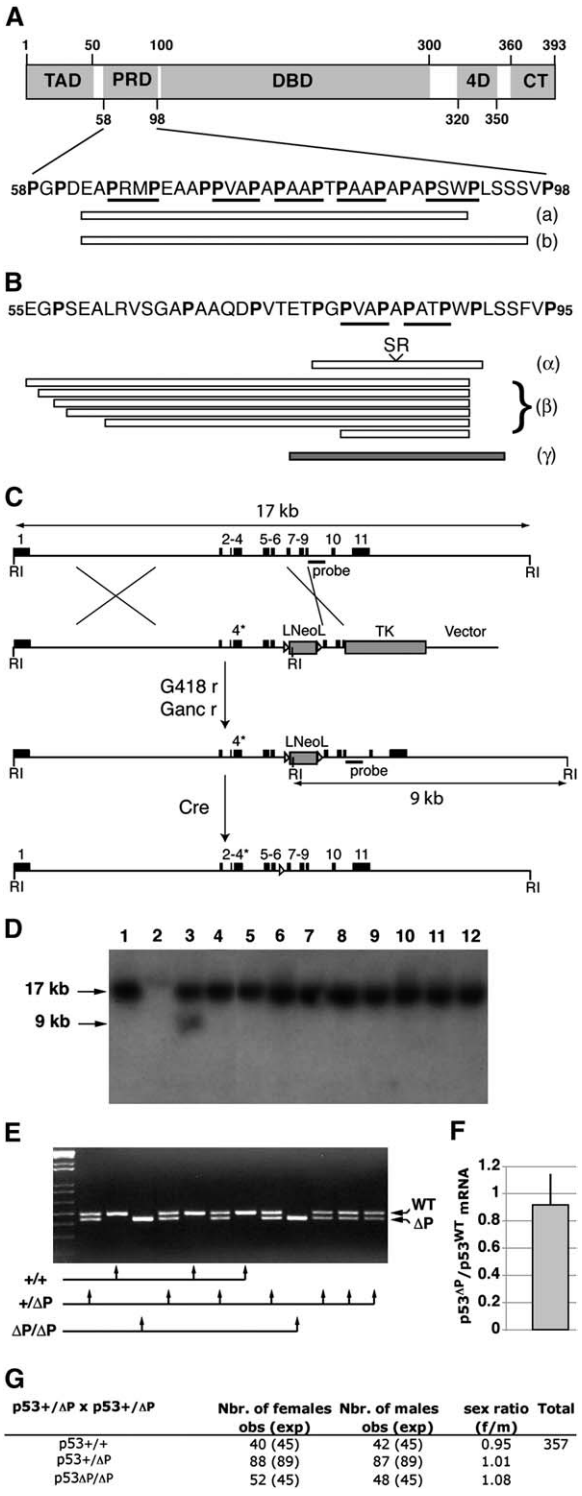

Figure 1. Targeting the p53$^{\Delta P}$ mutation at the mouse *p53* locus

A: Human p53 is a protein of 393 amino acids with five proposed domains: the transactivation (TAD), proline-rich (PRD), specific DNA binding (DBD), tetramerization (4D), and C-terminal regulatory (CT) domains. The human PRD is detailed below, with prolines (P) in bold and PXXP motifs underlined. Empty boxes: residues deleted in p53$^{\Delta P}$ mutants from (a) Walker and Levine (1996); (b) Hengstermann et al. (1998).

B: Residues 55–95 of murine p53 are shown, with prolines and PXXPs as in **A**. Empty boxes: residues deleted in p53$^{\Delta P}$ mutants from (α) Sakamuro et al. (1997) (with an additional insertion of two residues); (β) Edwards et al. (2003). Gray box (γ): residues deleted here.

but not apoptosis (Baptiste et al., 2002; Chipuk et al., 2004; Roth et al., 2000; Sakamuro et al., 1997; Venot et al., 1998; Zhu et al., 1999) and proposed that p53$^{\Delta P}$ transactivates *p21* but not crucial proapoptotic genes (Roth et al., 2000; Venot et al., 1998). An alternative would be that p53$^{\Delta P}$ cannot induce transcription-independent apoptosis because it does not bind Bcl-xL (Chipuk et al., 2004). Taken together, the data suggest that the PRD may be a molecular switch that enables p53 to induce either apoptosis or cell cycle arrest.

Further analysis of p53$^{\Delta P}$ could give insight into the regulation of p53 by its negative regulators, Mdm2 and Mdm4, as the precise mechanisms remain controversial. Deficiency of either Mdm2 or Mdm4 results in early embryonic lethality, which is rescued by loss of p53. Mdm2 deficiency leads to death ~3.5 days post coitum (dpc), due to elevated apoptosis (Jones et al., 1995; Montes de Oca Luna et al., 1995) that is partially rescued by Bax deficiency (Chavez-Reyes et al., 2003). Mdm4 deficiency causes lethality later, apparently by cell proliferation arrest (Finch et al., 2002; Migliorini et al., 2002; Parant et al., 2001) that is partially rescued by p21 loss (Steinman et al., 2004). The differences in timing and cause of embryonic lethality led to the proposal that Mdm2 and Mdm4 regulate nonoverlapping p53 functions, with Mdm2 regulating apoptosis and Mdm4 regulating cycle arrest (Parant et al., 2001). However, Mdm4 was soon after shown to regulate apoptosis in some tissues in vivo (Finch et al., 2002; Migliorini et al., 2002). Another model to explain the inability of either regulator to compensate for the loss of the other postulates an interdependent relationship in which Mdm4 stabilizes Mdm2, while Mdm2 enables nuclear import of Mdm4 (Gu et al., 2002). While the results of one study were consistent with this model (Gu et al., 2002), later studies disagreed (Danovi et al., 2004; Linares et al., 2003). Thus, the important questions of whether Mdm4 and Mdm2 are interdependent, and how they control p53, remain unanswered.

We generated mice in which the p53 PRD was deleted to gain insight into its functional contributions under conditions that maintain physiologically relevant levels of p53 pathway components. This is critical, as altering the level of Mdm2 relative to p53$^{\Delta P}$ profoundly affects the stability and transactivation ability of this mutant (Berger et al., 2001; Dumaz et al., 2001). Most p53$^{\Delta P}$ studies have been performed on human p53. Since the PRD is loosely conserved, the deletion we introduced was based on a study showing that a deletion of six prolines and

C: Targeting strategy. The 11 exons of wild-type *p53* are contained in a 17 kb EcoRI fragment. The targeting construct (below) contains: a 5′ homology region (with exons 1–6; 4* designates the mutated exon), a floxed Neo gene (LNeoL), a 3′ homology region (exons 7–9), and a Thymidine Kinase gene (TK). Targeted recombinants are G418 and gancyclovir resistant, result from the described crossing-overs, and are detected by Southern blot with the indicated probe as containing a 9 kb band. Cre expression in the male germline subsequently allows excision of Neo.

D: ES clones analyzed as described in **C**. Clone 3 contains a wild-type 17 kb fragment and a recombinant 9 kb fragment.

E: Mouse genotyping by PCR. The mutant product (ΔP) is shorter by 51 bp.

F: p53 mRNAs were quantified in wild-type and *p53*$^{\Delta P/\Delta P}$ cells using real-time PCR, normalized to control mRNA levels, and the ratio of p53$^{\Delta P}$/p53^{WT} mRNA was determined. Results are from three independent experiments. Error bar represents SD.

G: Distribution of the offspring from intercrosses of *p53*$^{+/\Delta P}$ mice. Obs: observed; exp: expected numbers assuming a Mendelian distribution without sex distortion. The distribution conforms to expected values ($\upsilon = 5$; $\chi^2 = 2.19 < 15.09$).

both PXXPs of murine p53 induced cell cycle arrest but not apoptosis, as observed for human $p53^{\Delta P}$ (Sakamuro et al., 1997; Figure 1B). The analysis of the $p53^{\Delta P}$ mutant mouse we generated challenges the $p53^{\Delta P}$ phenotype identified from many transfection studies, provides insight into Mdm2 and Mdm4 functions, and demonstrates in vivo that eliminating Mdm4 is required for optimal p53 activation and p53-mediated tumor suppression. Consequently, inhibiting both Mdm2 and Mdm4 should be considered a prime objective for anticancer strategies.

Results

Targeting of a $p53^{\Delta P}$ mutation in the mouse

We used homologous recombination in ES cells to delete six prolines and both PXXP motifs (Figures 1B and 1C; Figure S1 in the Supplemental Data available with this article online). The ES cells contain PrmCre, a Cre-recombinase transgene expressed specifically in spermatocytes (O'Gorman et al., 1997). Targeted recombinants were identified by Southern blot with a probe from intron 9 (Figure 1D), and single integration events were verified with a Neo probe (data not shown). Candidate clones were confirmed by PCR and injected into blastocysts to generate chimeric mice. PCR verified germline transmission of the mutation and was used to genotype the mouse colony (Figure 1E). We isolated RNA from $p53^{\Delta P/-}$ MEFs and sequenced the entire coding region: the $p53^{\Delta P}$ sequence was identical to the wild-type p53 ($p53^{WT}$) sequence except for the deletion of nucleotides encoding the PRD. The quantification of p53 mRNAs from wild-type and $p53^{\Delta P/\Delta P}$ MEFs demonstrated identical p53 transcription from both alleles (Figure 1F).

We intercrossed $p53^{+/\Delta P}$ mice to assess the role of $p53^{\Delta P}$ during development. Intercrosses of $p53^{+/-}$ mice lead to a reduced yield of $p53^{-/-}$ animals resulting from a defect in neural tube closure, most likely caused by defective apoptosis, leading to exencephaly and death in 25% of female $p53^{-/-}$ embryos (reviewed in Miller et al., 2000). By contrast, intercrossing $p53^{+/\Delta P}$ mice yielded no underrepresentation of female mutants (Figure 1G), suggesting that $p53^{\Delta P}$ retains enough proapoptotic activity to ensure normal neural tube formation.

$p53^{\Delta P}$ is a weak transactivator with increased sensitivity to Mdm2

$p53^{WT}$ and $p53^{\Delta P}$ were present at very low levels in unstressed cells, in which no or very faint nuclear signals were observed. Upon adriamycin (ADR) treatment, both accumulated in nuclei, but $p53^{\Delta P}$ appeared to accumulate less than $p53^{WT}$ (Figure 2A). $p53^{\Delta P}$ is a less efficient transactivator than $p53^{WT}$ and exhibits target gene-specific differences in efficiency: Mdm2 and PUMA mRNA were ~1.5 times lower in $p53^{\Delta P/\Delta P}$ than in wild-type ADR-treated MEFs, while p21 and Noxa mRNA levels were ~3-fold lower (Figure 2B). The reduced efficiency on the p21 promoter was so severe that p21 mRNA levels were similar in ADR-treated $p53^{\Delta P/\Delta P}$ MEFs and unstressed wild-type cells. Western blots confirmed that $p53^{\Delta P}$ accumulated 2-3 times less than $p53^{WT}$ after ADR, and that $p53^{\Delta P}$ is a less effective inducer of p21 than Mdm2 (Figure 2C). The reduced transcription response was not due to a difference in damage kinase-mediated phosphorylation of $p53^{\Delta P}$ (see Figure S2).

Since $p53^{\Delta P}$ was proposed to be more sensitive to Mdm2-mediated degradation than $p53^{WT}$ (Berger et al., 2001; Dumaz et al., 2001), we determined if the lower $p53^{\Delta P}$ protein levels after ADR treatment correlated with reduced protein stability. Because Mdm2 targets p53 for degradation by the proteasome, we first used MG132 to verify that inhibition of the proteasome increased $p53^{\Delta P}$ levels, and then Nutlin 3a, which prevents Mdm2-p53 interaction (Vassilev et al., 2004), to demonstrate that $p53^{\Delta P}$ degradation is Mdm2 dependent (Figure 2D). Direct evidence that $p53^{\Delta P}$ is more sensitive to Mdm2-mediated degradation than $p53^{WT}$ came from analysis of heterozygous MEFs in which the $p53^{WT}$ and $p53^{\Delta P}$ proteins are exposed to the same intracellular Mdm2 concentration. In these cells, $p53^{\Delta P}$ levels were four to five times less than $p53^{WT}$ (Figure 2E), and the half-life of $p53^{\Delta P}$ was significantly reduced (Figure 2F). Finally, we analyzed the effects of varying *Mdm2* gene copy number in $p53^{+/+}$, $p53^{+/\Delta P}$, and $p53^{\Delta P/\Delta P}$ cells: decreased Mdm2 increased $p53^{WT}$ accumulation only marginally but markedly increased $p53^{\Delta P}$ levels (Figure S3). Thus, $p53^{\Delta P}$ is stabilized after ADR treatment but is far more sensitive to Mdm2-mediated degradation than $p53^{WT}$.

Basal p53 levels were low in unstressed wild-type and $p53^{\Delta P/\Delta P}$ cells, but $p53^{\Delta P}$ abundance was similar to or higher than that of $p53^{WT}$ (see Figure 2C and below). This probably derives from the lower Mdm2 levels in unstressed $p53^{\Delta P/\Delta P}$ MEFs (Figures 2B and 2C). Following γ-irradiation, $p53^{\Delta P}$ was more abundant that $p53^{WT}$ at most time points, but $p53^{\Delta P}$ induced less Mdm2 and p21 (Figure 2G). Thus damage-specific effects were observed, as $p53^{\Delta P}$ accumulated less than $p53^{WT}$ after ADR (Figure 2C), but more than $p53^{WT}$ after irradiation (Figure 2G). Q-PCR clarified these data by revealing that $p53^{\Delta P}$ more robustly activates *Mdm2* after ADR compared to irradiation (see Figures 2H and 2B). Thus, $p53^{\Delta P}$ is exquisitely sensitive to Mdm2, and its accumulation relies on the level of Mdm2 generated by the activating stress.

We used chromatin immune precipitation (ChIP) to determine whether the stress- and gene-specific differential transactivation of *p21* and *Mdm2* resulted from promoter-specific binding differences. Although $p53^{\Delta P}$ transactivates *p21* less well than *Mdm2* after ADR (Figure 2B), it binds both target promoters similarly, and about two to three times less efficiently than $p53^{WT}$ (Figure 2I). Furthermore, the relative binding of $p53^{\Delta P}$ to the *Mdm2* promoter did not differ significantly after ADR or irradiation (Figure 2I), even though stress-specific differences in *Mdm2* transactivation were observed (Figures 2B and 2H). Thus, the differences in transactivation cannot be explained by differences in DNA binding. Rather, they may result from differential capacities in recruiting transcription factors and/or coactivators at promoters, as recently proposed for another p53 mutant exhibiting stress- and gene-specific differences (Johnson and Attardi, 2005).

$p53^{\Delta P/\Delta P}$ cells exhibit a deficient arrest response but retain a proapoptotic response

We next analyzed $p53^{\Delta P}$ function in cell cycle and apoptosis control. Consistent with the low p21 expression in stressed $p53^{\Delta P/\Delta P}$ cells (Figure 2), irradiation and ADR doses that induce cell cycle arrest in wild-type MEFs failed to arrest $p53^{\Delta P/\Delta P}$ MEFs (Figures 3A and 3B). Low p21 levels may also account for the inability of $p53^{\Delta P/\Delta P}$ cells to undergo replicative senescence (data not shown). The lack of developmental defects in $p53^{\Delta P/\Delta P}$ mice, however, suggested that $p53^{\Delta P}$ may be competent to induce apoptosis (Figure 1G). We tested this by analyzing

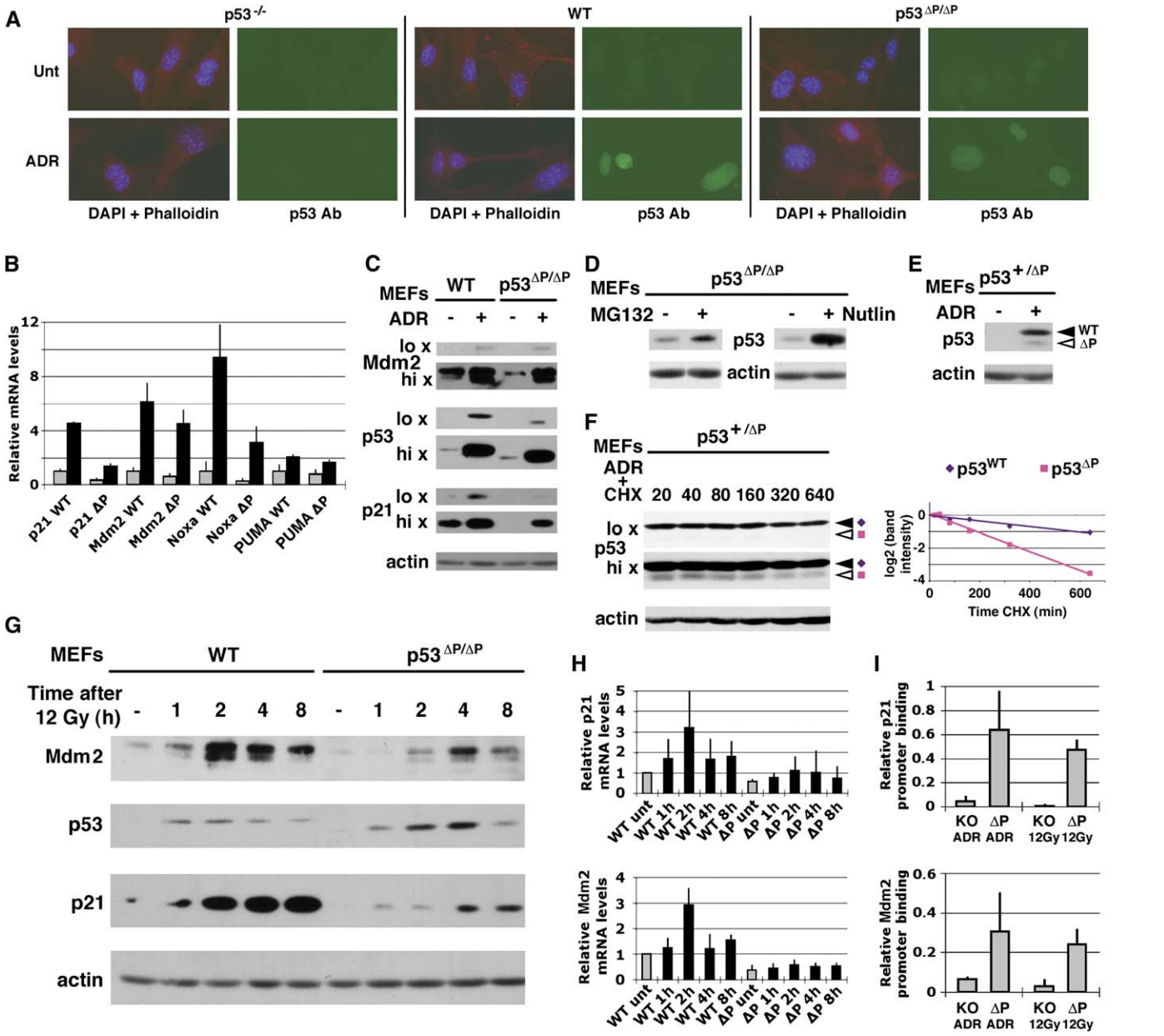

Figure 2. Accumulation and transactivation ability of p53$^{\Delta P}$ in response to DNA damage

A: *p53*$^{-/-}$, wild-type, and *p53*$^{\Delta P/\Delta P}$ MEFs were left untreated (Unt) or treated with adriamycin (ADR) at 0.5 μg/ml for 24 hr, then stained with antibodies against p53 (green) and phalloidin (red), and their DNA was counterstained with DAPI (blue).

B: RNAs from wild-type and *p53*$^{\Delta P/\Delta P}$ (ΔP) MEFs treated as in **A** were quantified using real-time PCR. Results are from three independent experiments. For each of the tested genes, the results were first normalized to control mRNA levels, then the mean amount of mRNAs in unstressed wild-type cells was assigned a value of 1. Gray bars: unstressed cells, Black bars: stressed cells. Error bars represent SD.

C: Wild-type and *p53*$^{\Delta P/\Delta P}$ MEFs were treated as in **A**, then protein extracts were immunoblotted with antibodies to Mdm2, p53, p21, and actin. Low/high exposures are designated lo x/hi x.

D: Extracts were prepared from *p53*$^{\Delta P/\Delta P}$ MEFs left untreated, or treated with 10 μM MG132 (left), or 10 μM Nutlin (right) for 4 hr.

E: *p53*$^{+/\Delta P}$ MEFs were treated and analyzed as in **C**.

F: p53$^{\Delta P}$ has a shorter half-life than p53^{WT} in *p53*$^{+/\Delta P}$ stressed MEFs. Cells were treated as in **A**, then incubated with cycloheximide (CHX) for the indicated times (in minutes). Graph shows half-life determinations. p53 bands were normalized to actin, then to the first time points. A decrease of one unit of $\log_2$ (band intensity) equals one half-life.

G: Wild-type and *p53*$^{\Delta P/\Delta P}$ MEFs were left untreated (−), or submitted to 12 Gy irradiation, and protein extracts were prepared 1, 2, 4, or 8 hr after irradiation.

H: RNAs from wild-type and *p53*$^{\Delta P/\Delta P}$ (ΔP) MEFs treated as in **G** were quantified and plotted as in **B**. Results are from three independent experiments. Error bars represent SD.

I: ChIP assay of p21 and Mdm2 promoters was performed in *p53*$^{-/-}$ (KO), wild-type, and *p53*$^{\Delta P/\Delta P}$ (ΔP) MEFs after ADR or 12 Gy γ-irradiation. For each stress condition, p53 bound response elements were purified with polyclonal antibody CM-5, quantified using real-time PCR, normalized to input DNA, then expressed as a fraction of bound response elements in wild-type cells (wild-type = 1). Results are from three (ADR) or two (γ-irradiation) independent experiments. Error bars represent SD.

MEFs sensitized to apoptosis by E1A overexpression (Lowe et al., 1993). An ADR dose that induced apoptosis in ~50% of wild-type MEFs (0.25 μg/ml) elicited little response in $p53^{\Delta P/\Delta P}$ cells, while higher ADR doses produced similar responses in wild-type and $p53^{\Delta P/\Delta P}$ cells (Figure 3C). Similarly, 2.5 μM etoposide induced apoptosis in ~50% of wild-type cells and few if any $p53^{\Delta P/\Delta P}$ cells, while 10 μM etoposide induced significant apoptosis in both genotypes. The low level of apoptosis in $p53^{-/-}$ cells under both conditions indicated that apoptosis was largely p53 dependent (Figure 3D). We next tested the apoptotic response of E1A MEFs after 6 or 12 Gy irradiation. About 25% of irradiated wild-type cells underwent apoptosis, while a significant, but reduced apoptotic response was observed *in* $p53^{\Delta P/\Delta P}$ cells (Figure 3E, left). However, we observed variations in the irradiation-induced apoptotic responses of $p53^{\Delta P/\Delta P}$ cells: few $p53^{\Delta P/\Delta P}$ cells were apoptotic in an experiment with 20% apoptotic wild-type cells (Figure 3E, right, black bars), while significant $p53^{\Delta P/\Delta P}$ apoptosis was observed in two experiments with 30% apoptotic wild-type cells (Figure 3E, right, gray bars). By contrast, significant apoptosis was never observed in irradiated $p53^{-/-}$ cells (Figure 3E). Apoptosis in irradiated $p53^{\Delta P/\Delta P}$ thymocytes in vivo was also variable: apoptotic $p53^{\Delta P/\Delta P}$ thymocytes were detected in an experiment with 50% apoptotic wild-type cells, but not in two experiments with 30% apoptotic wild-type cells, and apoptotic $p53^{-/-}$ cells were never detected (data not shown). In sum, $p53^{\Delta P}$ exhibits a measurable, but significantly compromised apoptotic response.

$p53^{\Delta P}$ rescues *Mdm4* null but not *Mdm2* null embryos

The embryonic lethalities resulting from Mdm2 or Mdm4 loss provide a powerful assay for analyzing the functionality of hypomorphic *p53* alleles. As $p53^{\Delta P}$ exhibited different capacities for apoptosis and cell cycle control, we determined if it exhibited a differential capacity to rescue lethality due to Mdm2 or Mdm4 deficiency. No $p53^{\Delta P/\Delta P}$ $Mdm2^{-/-}$ mice were observed from intercrosses of $p53^{\Delta P/\Delta P}$ $Mdm2^{+/-}$ mice (Table 1, upper), or from $p53^{+/\Delta P}$ $Mdm2^{+/-}$ intercrosses (data not shown). In striking contrast, viable $p53^{\Delta P/\Delta P}$ $Mdm4^{-/-}$ mice were obtained in Mendelian proportions from intercrosses of $p53^{\Delta P/\Delta P}$ $Mdm4^{+/-}$ (Table 1, lower) or $p53^{+/\Delta P}$ $Mdm4^{+/-}$ mice (data not shown). $p53^{\Delta P/\Delta P}$ $Mdm4^{-/-}$ mice did not exhibit overt phenotypic abnormalities.

Mdm4 deficiency augments $p53^{\Delta P}$ functions without affecting Mdm2 stability

The rescue of $Mdm4^{-/-}$ mice by $p53^{\Delta P}$ enabled analysis of the consequences of Mdm4 loss on p53 regulation in vivo. Mdm4 loss significantly decreased the proliferation rate of $p53^{\Delta P/\Delta P}$ cells (Figure 4A). Importantly, unlike $p53^{\Delta P/\Delta P}$ MEFs, irradiated $p53^{\Delta P/\Delta P}$ $Mdm4^{-/-}$ MEFs did arrest. However, the arrest response was still not as efficient as that observed in wild-type cells (Figures 4B and 3A). Consistent with a decreased proliferation rate and partially restored arrest response, p21 protein levels were elevated in both unstressed and ADR-treated $p53^{\Delta P/\Delta P}$ $Mdm4^{-/-}$ cells (Figure 4C). Mdm4 loss also resulted in higher Mdm2 levels and lower $p53^{\Delta P}$ levels after ADR (Figure 4C). Similarly, γ-irradiated $p53^{\Delta P/\Delta P}$ $Mdm4^{-/-}$ cells exhibited higher p21 and Mdm2 levels than $p53^{\Delta P/\Delta P}$ cells, and lower $p53^{\Delta P}$ levels at later time points (Figure 4D).

We tested whether the increased p21 and Mdm2 protein levels in $Mdm4^{-/-}$ cells resulted from increased transactivation by $p53^{\Delta P}$, since both are p53 target genes and Mdm4 has no p53-independent effects on cell proliferation or cycle control (Migliorini et al., 2002). Q-PCR analyses are consistent with this idea (Figure 4E). However, Mdm4 loss did not significantly increase the binding of $p53^{\Delta P}$ to the corresponding promoters (data not shown).

One model based on transfection studies is that Mdm4 stabilizes Mdm2 (Gu et al., 2002). According to this model, Mdm4 loss should destabilize Mdm2, leading to elevated p53 levels. As we did not observe this, we tested the model directly by comparing Mdm2 stability in the presence and absence of Mdm4. Strikingly, Mdm4 deficiency did not alter Mdm2 stability in unstressed or DNA damaged cells (Figure 4F).

Mdm2 and Mdm4 affect $p53^{\Delta P}$ function by different mechanisms

We varied *Mdm2* and *Mdm4* gene dosage in $p53^{\Delta P/\Delta P}$ MEFs to determine their relative contributions to p53 regulation. As $p53^{\Delta P/\Delta P}$ $Mdm2^{-/-}$ MEFs could not be isolated, we compared $p53^{\Delta P/\Delta P}$ $Mdm2^{+/-}$, $p53^{\Delta P/\Delta P}$ $Mdm4^{+/-}$, $p53^{\Delta P/\Delta P}$ $Mdm2^{+/-}$ $Mdm4^{+/-}$, and $p53^{\Delta P/\Delta P}$ $Mdm4^{-/-}$ MEFs. Each genotype partially restored the arrest response of $p53^{\Delta P}$ (Figures 5A and 4B). Western blots revealed that the loss of one *Mdm2* or *Mdm4* gene copy modestly increased p21 levels, cells heterozygous for both *Mdm2* and *Mdm4* expressed slightly more p21, and $Mdm4^{-/-}$ cells expressed the highest p21 levels (Figure 5B). Consistent with our previous observations (Figure 4), the $p53^{\Delta P}$ levels were decreased in stressed cells with only one or no *Mdm4* alleles, presumably because of their elevated Mdm2 levels. In contrast, $Mdm2^{+/-}$ cells exhibited lower Mdm2 levels correlating with a significant increase in $p53^{\Delta P}$ abundance (Figure 5B).

We gained insight into the mechanisms by which each negative regulator may function by analyzing how the induction of p21 varied with the amount of $p53^{\Delta P}$ present in cells of each genotype (Figure 5B). Reducing *Mdm2* gene dosage significantly increased $p53^{\Delta P}$ levels, compensating for the poor transactivation activity of $p53^{\Delta P}$ to generate higher p21 levels. By contrast, reduced *Mdm4* gene dosage resulted in significantly decreased $p53^{\Delta P}$ levels, yet $p53^{\Delta P}$ was able to induce p21 even more efficiently. Thus, in $Mdm4^{-/-}$ cells the elevated Mdm2 levels engendered more efficient $p53^{\Delta P}$ degradation, but the remaining $p53^{\Delta P}$ was a more efficient transcriptional activator.

$p53^{\Delta P}$ suppression of tumor growth is enhanced by reducing Mdm2 and Mdm4 expression, or by eliminating Mdm4

We compared spontaneous tumor onset in wild-type, $p53^{-/-}$, and $p53^{\Delta P/\Delta P}$ mice. While all $p53^{-/-}$ mice developed fatal tumors within 10 months, very few tumors were found after 12 months in $p53^{\Delta P/\Delta P}$ mice (Figure 6A). We detected thymic lymphomas and sarcomas in $p53^{\Delta P/\Delta P}$ mice, tumor types associated with p53 deficiency in mice (Donehower et al., 1992), but too few mice have been analyzed thus far to define a tumor spectrum. The delayed onset of spontaneous tumors in $p53^{\Delta P}$ mice is reminiscent of that of mice expressing $p53^{R172P}$ (also called $p53^{515C}$; Liu et al., 2004). The $p53^{R172P}$ mutant also retains only part of its tumor suppressor functions. However, the tumors that form later in these animals are very aggressive and grow rapidly. One hypothesis is that the enfeebled

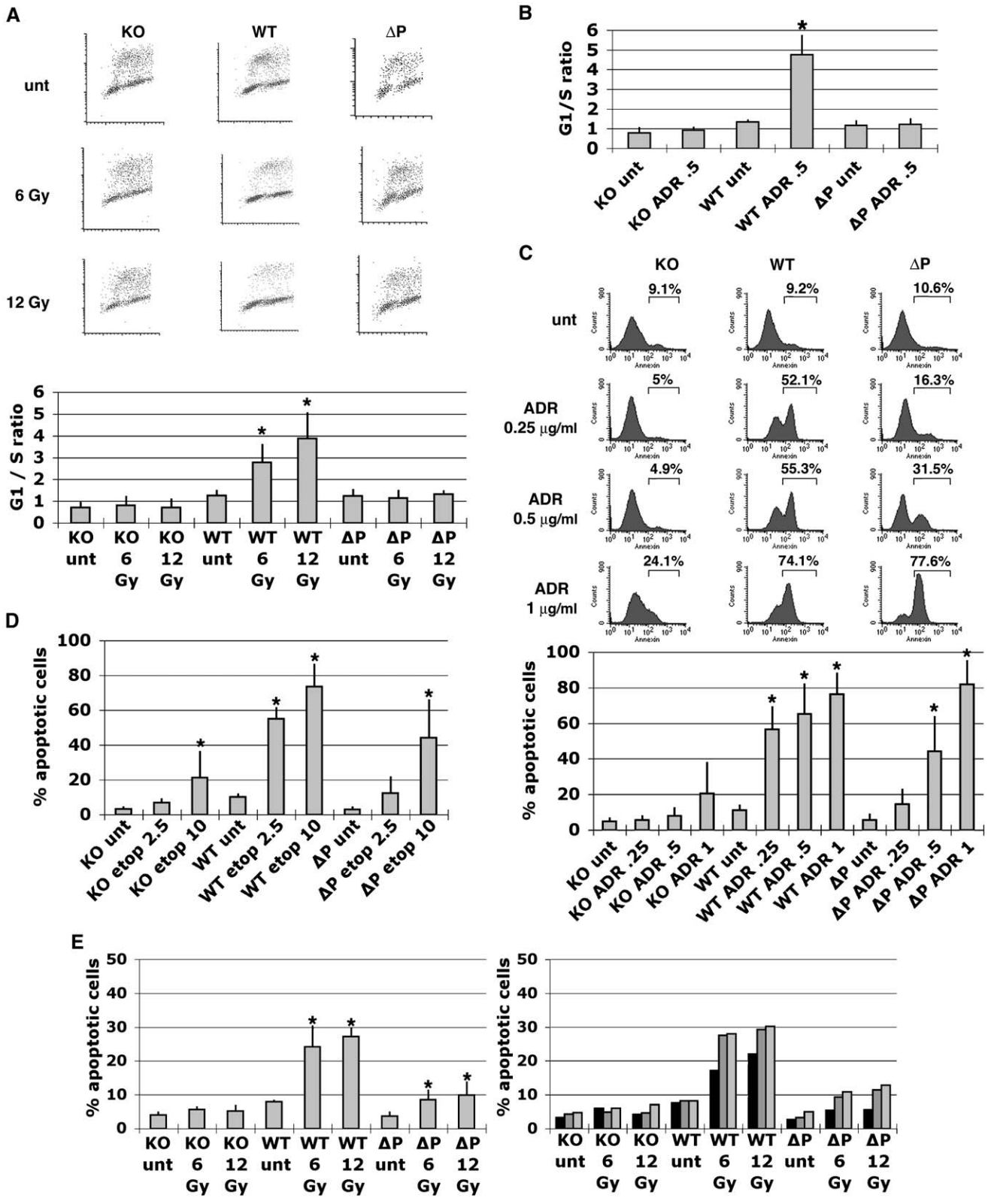

Figure 3. $p53^{\Delta P}$ does not induce cell cycle arrest but can induce apoptosis

A: Cell cycle control was analyzed in $p53^{-/-}$ (KO), wild-type, and $p53^{\Delta P/\Delta P}$ (ΔP) MEFs, in asynchronous cell populations left untreated, or 24 hr after 6 or 12 Gy γ-irradiation. On top, a typical experiment for cells of each genotype is shown. Results are from ≥8 independent experiments and ≥2 independent MEFs. Asterisks indicate significant differences after irradiation.

B: Cell cycle control was analyzed as in **A**, in asynchronous cell populations left untreated, or treated for 24 hr with 0.5 μg/ml ADR. Results are from four independent experiments.

$p53^{R172P}$ protein does not efficiently suppress tumor growth in clones where oncogenic events have occurred (Liu et al., 2004).

We tested if a similar situation applied to $p53^{\Delta P}$, by analyzing the ability of $p53^{\Delta P}$ to suppress oncogene-induced tumors. A constant number of E1A- and Ras-expressing (E1A + Ras) $p53^{+/+}$, $p53^{-/-}$, and $p53^{\Delta P/\Delta P}$ MEFs was injected into the flanks of nude mice, and the weights of age-matched tumors were compared after 10–15 days. E1A + Ras $p53^{-/-}$ cells generated large tumors in all mice, while E1A + Ras $p53^{+/+}$ did not. Importantly, E1A + Ras $p53^{\Delta P/\Delta P}$ cells showed very little, if any suppression of oncogene-induced tumor growth (Figure 6B). We also determined the ability of $p53^{\Delta P}$ to suppress oncogene-induced tumors in cells with reduced levels of Mdm2 and/or Mdm4. Half the gene dosage for either *Mdm2* or *Mdm4* improved tumor suppression marginally, if at all. However, decreasing the gene dosage for both *Mdm2* and *Mdm4* showed a 4-fold decrease in tumor size. Strikingly, the number and size of tumors generated from E1A + Ras $p53^{\Delta P/\Delta P}$ $Mdm4^{-/-}$ MEFs were similar to those from E1A + Ras $p53^{+/+}$ MEFs (Figure 6B). These data provide in vivo evidence that the specific inhibition of Mdm4 can dramatically improve tumor suppression.

Discussion

p53 is a transcription factor capable of inducing death, senescence, cell cycle arrest, or DNA repair. Complex regulatory mechanisms determine the appropriate response. The p53 N terminus plays an essential role in this regulation, with multiple N-terminal serines and threonines phosphorylated after damage, and at least two domains, the TAD and PRD, that contribute to Mdm2 and Mdm4 binding. Phosphorylation of the N-terminal serines was proposed to diminish Mdm2 binding while enhancing coactivator association. However, analyses of p53 serine-alanine mutants indicate that these residues are modulators of, rather than essential for, p53 activation (e.g., Chao et al., 2003). In sharp contrast, subtle changes in the levels of Mdm2 and Mdm4 can profoundly affect p53 activation and tumor suppression (Bond et al., 2004; this report). Recent studies also show that DNA damage induces phosphorylation of Mdm2 and Mdm4 to alter their stability and access to p53 (see below). In sum, factors that regulate the abundance, stability, and association of Mdm2 and Mdm4 with p53 combine to trigger a p53 response. This study employed genetic strategies in the mouse to show that the p53 PRD significantly contributes to Mdm2-mediated control of p53 stability, that Mdm2 and Mdm4 differentially regulate p53, and that Mdm4 inhibition can augment tumor suppression by p53.

$p53^{\Delta P}$, a hypomorphic protein exquisitely sensitive to Mdm2 control

Our study shows that a targeted PRD deletion made p53 more sensitive to Mdm2 (Figures 2E and 2F and Figure S3) and affected its ability to induce target genes (Figures 2B and 2C). Moreover, $p53^{\Delta P/\Delta P}$ cells were unable to induce cell cycle arrest but could induce apoptosis (Figure 3). This phenotype is surprising compared to that observed in many transfection studies (see Introduction). An inability to induce cell cycle arrest is readily explained by weak transactivation of *p21* by $p53^{\Delta P}$. Reducing Mdm2 or Mdm4 levels partially restored p21 induction and cell cycle arrest in $p53^{\Delta P/\Delta P}$ cells (Figures 4 and 5). This result emphasizes that, as for $p53^{WT}$, the balance between $p53^{\Delta P}$ and these two inhibitors is critical for proper p53 regulation. Accurate reproduction of the physiologic balance between p53, Mdm2, and Mdm4 is difficult to achieve by transfection, which could explain why the in vivo and transfection analyses generated different phenotypes. An additional important factor is that the endpoints of the PRD deletion can affect the ability of the mutant to induce an apoptotic response (Edwards et al., 2003). Taken together, we suggest that the PRD may have evolved to fine-tune Mdm2 (and possibly Mdm4) binding, which in turn impacts on stability control and transcriptional output. Analyses in progress will determine whether the PRD functions as a structural regulator dependent on proline isomerization (Mantovani et al., 2004), as a protein interaction domain such as PXXP (Dornan et al., 2003), or merely as a spacer between the TAD and the DNA binding domain.

Table 1. $p53^{\Delta P}$ rescues Mdm4 deficiency, but not Mdm2 deficiency

[a] $p53^{\Delta P/\Delta P}$ $Mdm2^{+/-}$ × $p53^{\Delta P/\Delta P}$ $Mdm2^{+/-}$	No. of mice: obs (exp)	Total
$p53^{\Delta P/\Delta P}$ $Mdm2^{+/+}$	23 (23)	93
$p53^{\Delta P/\Delta P}$ $Mdm2^{+/-}$	70 (47)	
$p53^{\Delta P/\Delta P}$ $Mdm2^{-/-}$	0 (23)	
[b] $p53^{\Delta P/\Delta P}$ $Mdm4^{+/-}$ × $p53^{\Delta P/\Delta P}$ $Mdm4^{+/-}$	No. of mice: obs (exp)	Total
$p53^{\Delta P/\Delta P}$ $Mdm4^{+/+}$	16 (23)	91
$p53^{\Delta P/\Delta P}$ $Mdm4^{+/-}$	53 (45)	
$p53^{\Delta P/\Delta P}$ $Mdm4^{-/-}$	22 (23)	

[a] Offspring from $p53^{\Delta P/\Delta P}$ $Mdm2^{+/-}$ intercrosses. Observed (obs) values differ from expected (exp) Mendelian ratios ($\upsilon = 2$; $\chi^2 = 35.13 > 9.21$).
[b] Offspring from $p53^{\Delta P/\Delta P}$ $Mdm4^{+/-}$ intercrosses. The distribution conforms to Mendelian expected values ($\upsilon = 2$; $\chi^2 = 3.46 < 9.21$).

Analysis of $p53^{\Delta P}$ regulation by Mdm2 and Mdm4 suggests an alternative model for p53 control

In a wild-type context, Mdm2 loss leads to embryonic death due to elevated apoptosis, while Mdm4-deficient embryos die mainly from cell proliferation arrest (see Introduction). It is striking that the compromised function of $p53^{\Delta P}$ fails to rescue Mdm2 loss but fully rescues Mdm4 deficiency (Table 1). The sensitivity of the hypomorphic $p53^{\Delta P}$ mutant to Mdm2 and Mdm4 also affords a larger dynamic range within which to evaluate their contributions to p53 stability and functional output.

C: E1A expressing $p53^{-/-}$, $p53^{+/+}$, and $p53^{\Delta P/\Delta P}$ MEFs were left untreated or treated with indicated doses of ADR for 24 hr. On top, a typical experiment for cells of each genotype is shown. Results are from ≥6 independent experiments and ≥2 independent MEFs. Asterisks indicate significant increases in apoptotic cells (apoptosis in a fraction of untreated cells (particularly in wild-type MEFs) most likely reflects mild stresses generated by E1A expression and cell culture).
D: Apoptosis was analyzed as in **C**, in E1A-expressing MEFs, untreated or treated with 2.5 or 10 μM etoposide for 24 hr. Results are from three independent experiments.
E: Apoptosis in untreated E1A-expressing MEFs or 24 hr after 6 or 12 Gy irradiation. Left shows results averaged from three independent experiments; right shows the individual experiments, respectively, in black bars, dark gray bars, and light gray bars.
Error bars indicate SD.

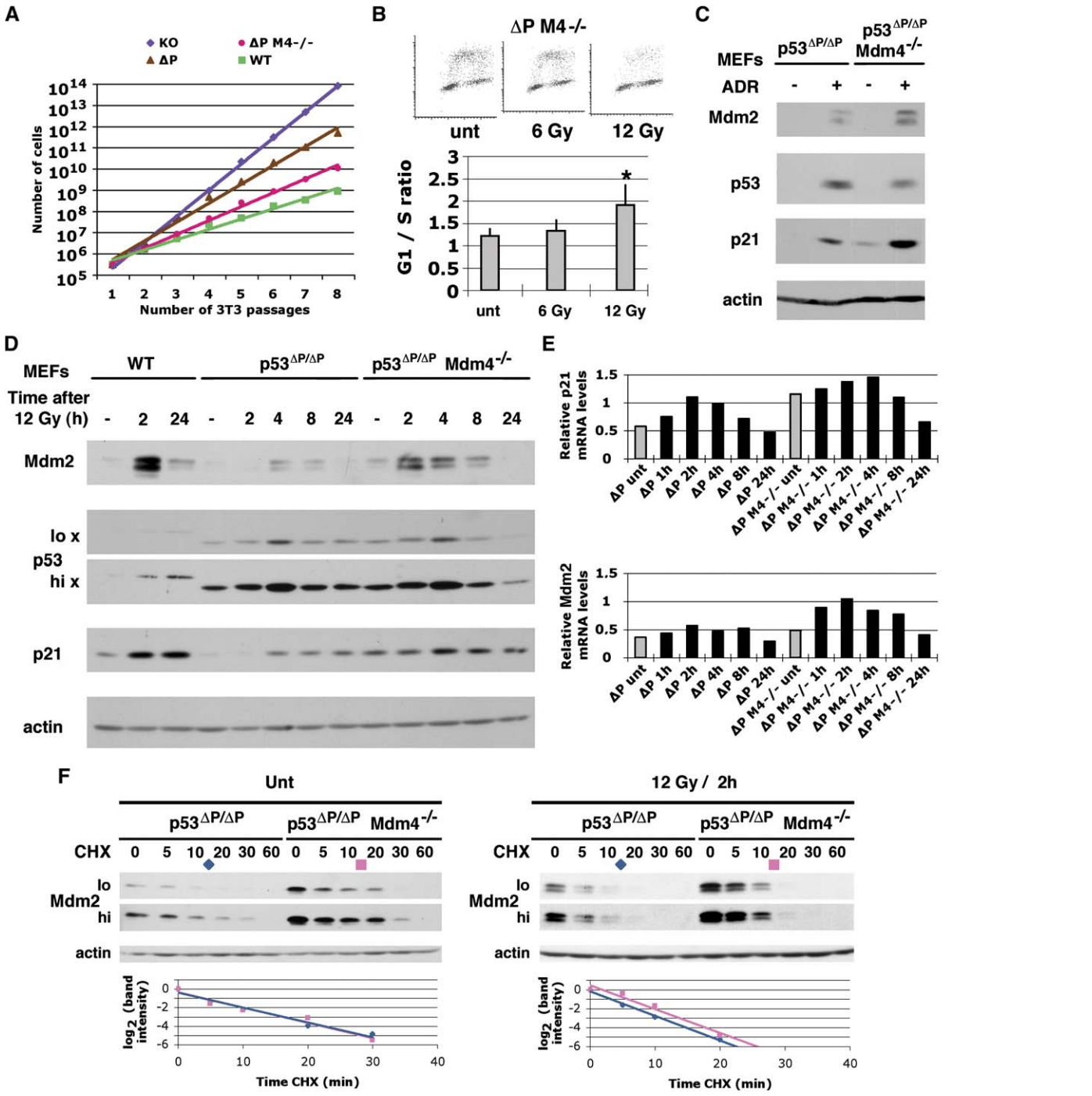

Figure 4. Consequences of the loss of Mdm4

A: The proliferation of $p53^{-/-}$ (KO), $p53^{\Delta P/\Delta P}$ (ΔP), $p53^{\Delta P/\Delta P}$ $Mdm4^{-/-}$ (ΔP M4−/−), and wild-type MEFs was compared using a 3T3 protocol. Each point is a mean value from two independent MEFs, the value for each MEF resulting from duplicate plates. Starting from 3×10^5 cells, 10^{12} $p53^{\Delta P/\Delta P}$ cells were obtained after eight passages, corresponding to ~22 cell doublings (cd; $3 \times 10^5 \times 2^{22} = 1.2 \times 10^{12}$). Only 10^{10} $p53^{\Delta P/\Delta P}$ $Mdm4^{-/-}$ MEFs were counted (~15 cd). Thus, Mdm4 loss slows down $p53^{\Delta P/\Delta P}$ cell doubling by ~30% (1 − 15/22 = 0.3).

B: Cell cycle arrest in $p53^{\Delta P/\Delta P}$ $Mdm4^{-/-}$ (ΔP M4−/−) MEFs was analyzed and plotted as in Figure 3A. Results are from two independent MEFs in ≥7 independent experiments. Error bars represent SD.

C: $p53^{\Delta P/\Delta P}$ and $p53^{\Delta P/\Delta P}$ $Mdm4^{-/-}$ MEFs were left untreated or treated with ADR as before.

D: Wild-type, $p53^{\Delta P/\Delta P}$, and $p53^{\Delta P/\Delta P}$ $Mdm4^{-/-}$ MEFs were left untreated (−), or submitted to 12 Gy irradiation, and protein extracts were prepared 2–24 hr after irradiation.

E: RNAs from $p53^{\Delta P/\Delta P}$ (ΔP) and $p53^{\Delta P/\Delta P}$ $Mdm4^{-/-}$ (ΔP M4−/−) MEFs treated as in **D** were quantified using real-time PCR and plotted as in Figure 3. Results are from three independent experiments.

F: Mdm2 half-life in $p53^{\Delta P/\Delta P}$ and $p53^{\Delta P/\Delta P}$ $Mdm4^{-/-}$ MEFs. Cells, unstressed or 2 hr after 12 Gy irradiation, were incubated with CHX for the indicated times (in minutes). For half-life determination, Mdm2 bands were normalized to actin, then to the first time point.

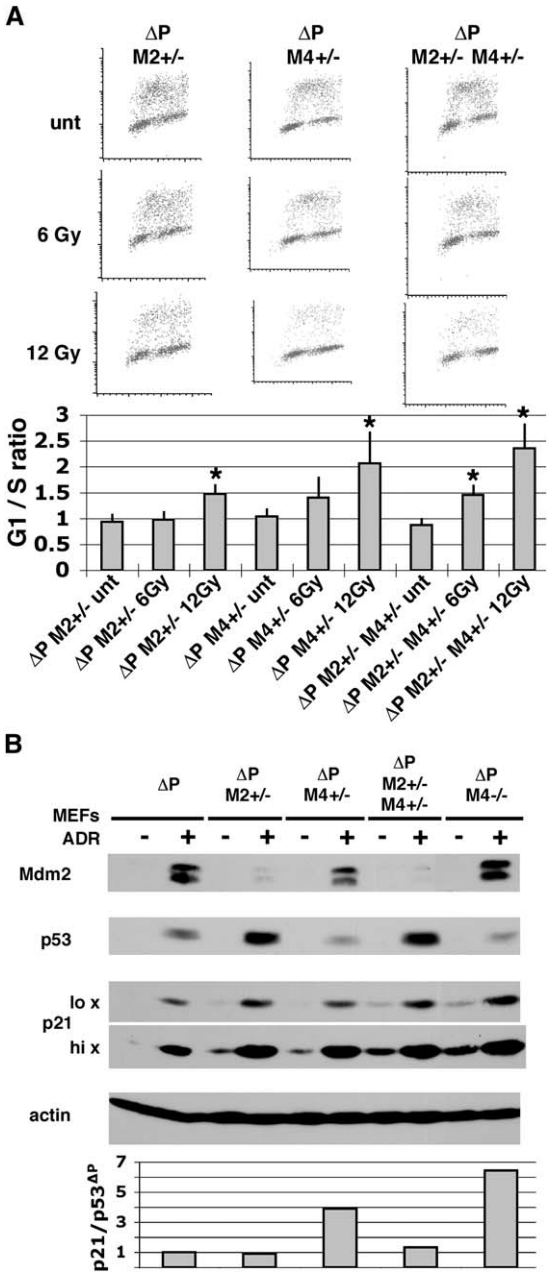

Figure 5. Effects on $p53^{\Delta P}$ of a reduction in *Mdm4* and/or *Mdm2* gene dosage

A: Cell cycle arrest in $p53^{\Delta P/\Delta P}$ $Mdm2^{+/-}$ (ΔP M2+/−), $p53^{\Delta P/\Delta P}$ $Mdm4^{+/-}$ (ΔP M4+/−), and $p53^{\Delta P/\Delta P}$ $Mdm2^{+/-}$ $Mdm4^{+/-}$ (ΔP M2+/− M4+/−) MEFs was analyzed and plotted as in Figure 3A. Results are, for each genotype, from two independent MEFs in ≥7 independent experiments. Error bars represent SD.
B: $p53^{\Delta P/\Delta P}$, $p53^{\Delta P/\Delta P}$ $Mdm2^{+/-}$, $p53^{\Delta P/\Delta P}$ $Mdm4^{+/-}$, $p53^{\Delta P/\Delta P}$ $Mdm2^{+/-}$ $Mdm4^{+/-}$, and $p53^{\Delta P/\Delta P}$ $Mdm4^{-/-}$ MEFs were left untreated or treated with ADR as before. The graph below indicates the ratio between band intensities for p21 and $p53^{\Delta P}$ in stressed cells of each genotype, with a value of 1 assigned to the ratio in $p53^{\Delta P/\Delta P}$ cells.

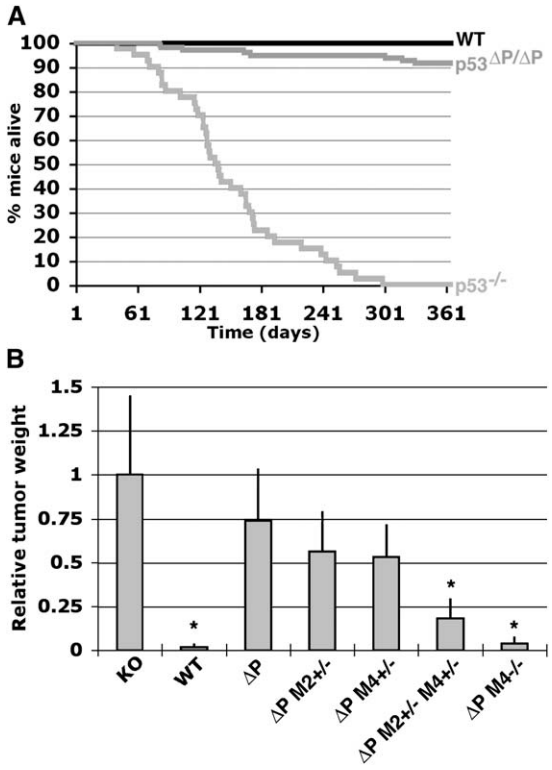

Figure 6. $p53^{\Delta P}$ delays the onset of spontaneous tumors but is a poor suppressor of oncogene-induced tumor xenografts

A: The cumulative survival of wild-type, $p53^{\Delta P/\Delta P}$, and $p53^{-/-}$ mice after 1 year was compared. Data are from ≥40 animals for each genotype. Cause-specific survival was used; mice affected by causes other than tumors were censored.
B: E1A + Ras xenograft assay. Results are expressed as the relative weight of age-matched tumors, with a value of 1 given to the average weight from $p53^{-/-}$ cells. Results are from ≥7 tumors for each genotype. Asterisks note tumor sizes significantly lower than that from $p53^{\Delta P/\Delta P}$ cells. Error bars represent SD.

Western analyses showed that deleting even a single copy of *Mdm2* significantly increased $p53^{\Delta P}$ levels, leading to increased transactivation of p53 target genes (Figure 5B). We infer that total absence of Mdm2 allows $p53^{\Delta P}$ to accumulate sufficiently to exceed Mdm4, resulting in continuous activation of cell cycle arrest and apoptotic genes to induce lethality. In addition, extremely high $p53^{\Delta P}$ levels could participate in a transcription-independent apoptosis response. By contrast, total loss of Mdm4 resulted in less abundant, but more active $p53^{\Delta P}$ (Figures 4 and 5B). Lower $p53^{\Delta P}$ levels would be unlikely to induce transcription-independent apoptosis. More importantly, in the absence of Mdm4, $p53^{\Delta P}$ activated more Mdm2 (Figures 4 and 5B). This Mdm2 had unfettered access to $p53^{\Delta P}$, creating the classic Mdm2-p53 negative feedback loop. In MEFs, Mdm4 deficiency in a $p53^{\Delta P/\Delta P}$ background increased p21 levels, but the levels were clearly inadequate to arrest embryonic development. It is possible that reducing p21 to an acceptable level explains how $p53^{\Delta P}$ fully rescues Mdm4 loss, since total absence of p21 merely delays death and shifts the cause of lethality from proliferation arrest to apoptosis (Chavez-Reyes et al., 2003; Steinman et al., 2004). Another explanation is that $p53^{\Delta P}$, due to its higher sensitivity to Mdm2, may fail to activate additional target genes that contribute to lethality in $p53^{WT}$ animals lacking Mdm4.

In a $p53^{WT}$ context, the death of both Mdm2- and Mdm4-deficient mice indicated that each inhibitor is normally unable to compensate for the loss of the other. Two models were proposed to explain this observation. One postulates that Mdm2 and Mdm4 regulate nonoverlapping functions of p53, with

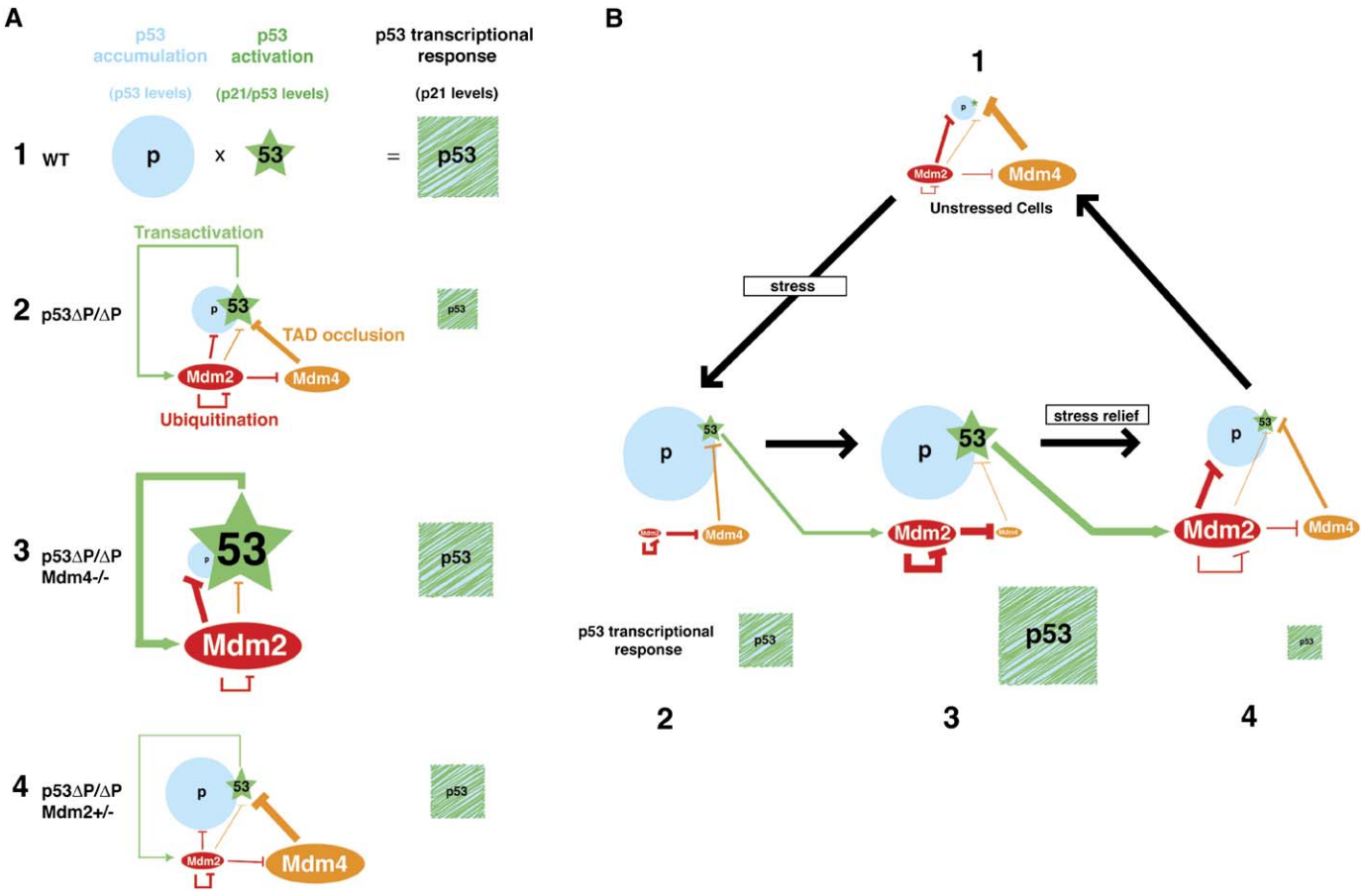

Figure 7. The p53$^{\Delta P}$ mutant suggests two different roles for Mdm2 and Mdm4 in controlling p53 function

A: Information gained by analyzing p53$^{\Delta P}$ in different *Mdm2* and *Mdm4* genetic contexts. p53$^{\Delta P}$ and p21 levels after ADR (Figures 2, 4, and 5) were used to estimate p53 stability and activity. **A1:** The transcriptional response (blue/green striped square) is the product of p53 accumulation (blue circle) by p53 activation (green star). Relative values for these parameters in wild-type cells are diagrammed for reference. **A2:** p53$^{\Delta P}$ accumulation and activation in *p53*$^{\Delta P/\Delta P}$ cells. The accumulation of p53$^{\Delta P}$ is 1/3, and the transcriptional response 1/4 of that observed in wild-type cells (Figure 2). The sizes of the circle, star, and square vary accordingly. Mdm2-Mdm4-p53 interactions are represented to enable comparisons below. This is a simplified view, in that only the overall interactions of the three proteins are drawn, rather than the dynamics of their interactions with each other or other proteins. The data suggest that Mdm4 is an important inhibitor of p53$^{\Delta P}$ activity (by TAD occlusion; orange), while Mdm2 mainly regulates p53$^{\Delta P}$ accumulation (through ubiquitination; red). Mdm2 also targets itself and Mdm4 for degradation, which we suggest is important to initiate/strengthen the p53 response (see **B**). Activated p53$^{\Delta P}$ transactivates Mdm2 (green) to establish a negative feedback loop. **A3:** Effects of Mdm4 deficiency on p53$^{\Delta P}$. The p53$^{\Delta P}$ response is increased, through a combined decreased p53$^{\Delta P}$ accumulation and increased p53$^{\Delta P}$ activation (Figures 4 and 5). As Mdm2 stability is independent of Mdm4 (Figure 4), the increased Mdm2 levels limit p53$^{\Delta P}$ accumulation. Mdm4 would play a predominant role in TAD occlusion, since p53$^{\Delta P}$ activity is higher in *Mdm4*$^{-/-}$ cells despite increased Mdm2 levels. The increased p53$^{\Delta P}$ transcriptional response remains lower than that observed in wild-type cells (striped squares, Figure 4), accounting for *p53*$^{\Delta P/\Delta P}$ *Mdm4*$^{-/-}$ mice viability. **A4:** Effects of reduced Mdm2 on p53$^{\Delta P}$. The p53$^{\Delta P}$ response is increased through an increase in p53$^{\Delta P}$ accumulation and a modest decrease in p53$^{\Delta P}$ activation (Figure 5). Reduced Mdm2 reduce p53$^{\Delta P}$ degradation, leading to increased p53$^{\Delta P}$ accumulation, but the reduced Mdm2 also compromises Mdm4 degradation, mitigating p53$^{\Delta P}$ activation.

B: A dynamic model of the p53 response that takes into account the relative contributions of Mdm2 and Mdm4 to p53 regulation. **B1:** In unstressed cells, p53 is kept at low levels (due to Mdm2-mediated ubiquitination) and inactive (due primarily to Mdm4-mediated TAD occlusion). (For simplicity, we have not included the effects of ATM, Chk2, or HAUSP, discussed in Marine and Jochemsen [2005].) **B2:** Upon stress, Mdm2 degrades itself and Mdm4, leading to the accumulation and activation of p53. **B3:** As activated p53 transactivates Mdm2, the increasingly abundant Mdm2 degrades Mdm4 more efficiently, allowing full p53 activation. **B4:** Upon stress relief, the accumulated Mdm2 now preferentially targets p53, which decreases p53 levels to potentially enable cell cycle reentry.

Mdm2 regulating apoptosis and Mdm4 regulating cell cycle arrest (Parant et al., 2001). The other proposes a mutual dependence of the regulators, in which Mdm4 stabilizes Mdm2 and Mdm2 enables nuclear import of Mdm4 (Gu et al., 2002). We showed that loss of one copy of *Mdm2*, or of one or both *Mdm4* alleles, increased p21 levels and partially restored cycle control. This observation, together with data indicating that Mdm4 can regulate apoptosis (Finch et al., 2002; Migliorini et al., 2002; Xiong et al., 2006; Francoz et al., 2006) or that Mdm2 overexpression can rescue Mdm4 loss (Steinman et al., 2005), is difficult to reconcile with the model of nonoverlapping p53 functions. Our data also clearly show that loss of Mdm4 does not alter Mdm2 stability (Figure 4F), in clear contrast to the predictions of the mutual dependency model. In fact, because Mdm4 loss translates into a relative decrease in p53$^{\Delta P}$ levels after damage, our results further suggest that Mdm2 does not require Mdm4 to regulate its own stability, or the stability of p53$^{\Delta P}$.

Our results suggest a third model in which Mdm2 and Mdm4 contribute in distinctly different ways to p53 control. We found that Mdm4 loss significantly activates $p53^{\Delta P}$ (Figure 5B). The observation that Mdm4 is produced at constant levels and binds the p53 TAD in the same region as Mdm2 suggests that Mdm4 functions to antagonize p53 activity under nonstressing conditions when Mdm2 levels are low (Marine and Jochemsen, 2005). Here, we observed higher $p53^{\Delta P}$ activity in stressed $Mdm4^{-/-}$ cells, indicating that $p53^{\Delta P}$ inhibition by Mdm4 is not restricted to unstressed conditions. As Mdm2 levels oscillate during the DNA damage response (Lev Bar-Or et al., 2000), the ratio between Mdm4 and Mdm2 should also vary during a stress response, which may account for our observation. Importantly, our data also show that the elevated $p53^{\Delta P}$ present in cells with reduced Mdm2 expression is markedly less active on a per molecule basis than $p53^{\Delta P}$ in cells lacking Mdm4. Even more surprising was our finding that $p53^{\Delta P}$ does not appear more active, on a per molecule basis, in $p53^{\Delta P/\Delta P}$ $Mdm2^{+/-}$ cells than in $p53^{\Delta P/\Delta P}$ cells (Figure 5B). Our data thus suggest a functional complementarity of Mdm2 and Mdm4, in which Mdm4 acts as a major inhibitor of p53 transcriptional activity, while Mdm2 mainly regulates p53 stability. Importantly, while this manuscript was under revision a similar conclusion was derived from studies using conditional activation of a $^{LoxStopLox}p53$ allele (Francoz et al., 2006). This indicates the relevance of the $p53^{\Delta P}$ mutant for understanding regulation of wild-type p53.

The observation that decreased Mdm2 levels stabilize but do not activate $p53^{\Delta P}$ seems paradoxical, because the classic negative feedback loop postulates that Mdm2 regulates p53 stability through ubiquitination, and activity by binding the p53 TAD. However, several recent reports reveal another role for Mdm2 in p53 control: Mdm2 auto-degradation and Mdm2-dependent degradation of Mdm4 after DNA damage (Chen et al., 2005; Kawai et al., 2003; Meulmeester et al., 2005; Okamoto et al., 2005; Pereg et al., 2005; Stommel and Wahl, 2004). The degradation of both negative regulators is critical for p53 activation, as proteasome inhibition prevents DNA damage from activating p53 (Stommel and Wahl, 2004). Thus, Mdm2 is required to both inhibit p53 in the classic negative feedback loop, and to also activate p53 through a positive process involving accelerated degradation of itself and Mdm4 after stress. We suggest that engagement by the proteasome makes both inhibitors less available for p53 binding, which facilitates p53 activation and accumulation. This model could explain why decreasing Mdm2 levels appears to have little effect on $p53^{\Delta P}$ activity: in $Mdm2^{+/-}$ cells, less Mdm2 would bind the p53 TAD, but Mdm4 would be degraded less efficiently. According to this, only when sufficient Mdm4 is degraded by Mdm2 does p53 become fully activated. Our findings and the p53 regulation model they suggest are summarized in Figure 7.

Augmenting $p53^{\Delta P}$ tumor suppression by Mdm4 deficiency: Implications for anticancer strategies

Given that $p53^{\Delta P}$ is a modest transactivator, we were surprised to find that it suppresses spontaneous tumor formation rather effectively (Figure 6A). On the other hand, it is a poor suppressor of oncogene-induced tumorigenicity in a xenograft model (Figure 6B). These observations may be explained in two ways. First, $p53^{\Delta P}$ resembles the $p53^{R172P}$ DNA binding domain mutant in that both induce a subset of p53 functions related to tumor suppression, but the latter exhibited a functional output opposite of $p53^{\Delta P}$ in that it induced cell cycle arrest and not apoptosis (Liu et al., 2004). Yet, like $p53^{\Delta P}$, $p53^{R172P}$ delayed tumor onset. It is possible that a subset of p53 output is required to suppress spontaneous tumor formation, but a more complete response is required in more advanced stages, when a collection of potent oncogenic mutations have occurred. A second possibility is that classic p53 target genes that regulate apoptosis and cell cycle control are not those that contribute most to preventing initiation of spontaneous tumors. We also observed that reducing the gene dosage of either *Mdm2* or *Mdm4* marginally affected the growth of oncogene-induced tumors. However, far more significant effects were observed by decreasing the expression of both regulators, or by the absence of Mdm4 activity (Figure 6B).

Inhibiting the interaction between p53 and Mdm2 has been recognized as an attractive anticancer strategy for many years. Several approaches revealed that antibodies and small molecules that bind Mdm2 in its p53 binding pocket may stabilize p53 and activate the p53 pathway (Vassilev et al., 2004 and references therein). Because the p53 binding domains of Mdm2 and Mdm4 are similar, these reagents might also antagonize Mdm4 binding, though it is unclear to what extent. We note that Mdm2 binding to p53 is stabilized by a ''lid'' that differs significantly in Mdm4 (McCoy et al., 2003). Consequently, optimal Mdm2 antagonists may not be optimal Mdm4 antagonists, as exemplified by SuperTip 12/1, which antagonizes Mdm2 11 times more efficiently than Mdm4 (Bottger et al., 1999). The search for optimal Mdm4 antagonists is clinically important, since Mdm4 amplification and overexpression occur in 20% of lung, breast, and colon tumors, the three most common human cancers (Danovi et al., 2004). In addition, our results provide both the rationale and experimental evidence that optimal antagonists to Mdm2 and Mdm4 could synergize to ensure strong p53 activation in tumors.

Experimental procedures

Targeting construct

Mouse genomic wild-type *p53* DNA was obtained from combining a 17 kb EcoRI fragment (from L. Donehower) and a 6 kb BamHI fragment (from T. Jacks). A 0.7 kb XhoI-XbaI fragment containing exon 4 was subcloned and mutated as described in Figure S1.

Targeting/genotyping

PrmCre 129/SvJae embryonic stem (ES) cells were electroporated with the targeting construct linearized with NotI. Of 197 G-418 and ganciclovir-resistant ES clones, two candidates were identified by Southern blot, confirmed by PCR (primer sequences available upon request), and injected into blastocysts. Germline transmission was verified by genotyping MEFs from breedings of chimeras with $p53^{+/-}$ mice. RT-PCR of RNAs from $p53^{\Delta P/-}$ MEFs showed that the mutant cDNA differed from the $p53^{WT}$ sequence only by the deletion of nucleotides encoding aa 75–91 (sequence available upon request). Mouse mutants KO for *p53* (Taconic), *Mdm2* (kind gift of G. Lozano), and *Mdm4* (kind gift of S.N. Jones) were genotyped according to published protocols. All experiments were performed according to IACUC regulations.

Cells and reagents

Primary MEFs were isolated from 13.5 day embryos, genotyped, and cultured, unless noted otherwise, for a maximum of four passages in DMEM with 15% FBS, 2-mercaptoethanol (100 mM), L-glutamine (2 mM), and antibiotics. Cells were γ-irradiated at RT with a 60 Co γ-irradiator, or treated with ADR, etoposide, MG132, or Nutlin 3a (kind gift of L. Vassilev). For half-life determinations, cells were treated with 100 μg/ml cycloheximide.

Immunofluorescence

MEFs were cultured on collagen-coated coverslips, exposed to ADR, and analyzed 24 hr later. Coverslips were stained with the p53 antibody CM-5 (Novacastra) and secondary antibodies Alexa Fluor 488 goat-α-mouse IgG2A and Alexa Fluor 568 goat-α-rabbit (Molecular Probes). Images were captured on an epifluorescence microscope using equal exposure times for all images for each fluor.

Western blots

Protein lysates were prepared and analyzed on SDS-PAGE gels as described (Stommel and Wahl, 2004). Blots were probed with primary antibodies against p53 (CM-5), p53 phospho-serine 18 (Cell Signaling Technologies), Mdm2 (2A10), p21 (C-19, Santa Cruz), and α-actin (Sigma). Peroxidase-conjugated secondary antibodies were detected using Pierce Supersignal West Pico chemiluminescent substrate. NIH Image 1.63 was used for band density quantification.

Q-PCR

Total RNA was extracted using RNeasy mini kit (Qiagen) and reverse transcribed using Superscript III RT (Invitrogen). Real-time quantitative PCR was performed on an ABI PRISM 7700 system using Platinum SYBR Green mastermix. Primer sequences for detecting cDNA sequence of p53, p21, Mdm2, Noxa, PUMA, and ARP and PPIA are available upon request.

ChIP assay

The procedure for ChIP assay was detailed recently (Nister et al., 2005).

Retrovirus preparation and infection of MEFs

Cells were infected with the pWZL-E1A12S virus, or were sequentially infected with pWZL-E1A12S and pBABE-HrasV12 viruses as previously described (Krummel et al., 2005). Importantly, populations of E1A- or E1A + Ras-expressing cells were used in all analyses, not individual clones, to minimize potential differences in expression levels that could result from independent viral insertion sites.

Flow cytometry

For cell cycle analysis, log phase cells were irradiated with 6 or 12 Gy γ-irradiation and incubated for 24 hr, or treated for 24 hr with ADR. Cells were then pulse labeled for 1 hr with BrdU (10 μM), fixed in 70% ethanol, and double stained with FITC anti-BrdU and propidium iodide, then analyzed as described (Krummel et al., 2005). Apoptosis assays were performed on E1A-expressing MEFs irradiated with 6 or 12 Gy γ-irradiation and incubated for 24 hr, or treated for 24 hr with ADR or etoposide, then harvested, stained with annexin V-FITC and analyzed using Facscan.

Tumorigenicity

Spontaneous tumor onset was determined in mice of $\geq$75% C57Bl/6 background. All mice in the cohort were >1 year old when survival curves were plotted. For oncogene-induced tumor assays, we injected 5×10^6 E1A + Ras-expressing MEFs of the different genotypes subcutaneously into the rear flank of 6-week-old female athymic nude mice. After 10–15 days, mice were sacrificed and tumors were isolated and weighed. All experiments were performed according to IACUC regulations.

Statistical analyses

Offspring were compared to Pearson χ^2 distribution tables with appropriate degrees of freedom (υ) and 99% confidence (details upon request). For QPCR, ChIP, cell cycle, apoptosis, and xenograft tumor assays, means ± SD are shown.

Supplemental data

The Supplemental Data include three supplemental figures and can be found with this article online at http://www.cancercell.org/cgi/content/full/9/4/273/DC1/.

Acknowledgments

We thank G. Lozano and S.N. Jones for *Mdm2* and *Mdm4* mutant mice, T. Jacks for a *p53* genomic clone, L. Vassilev for Nutlin, S. Lowe for retroviruses, G. Campbell and B. Jaroszynski for technical assistance, and S. O'Gorman and J. Chipuk for technical advices. The work was supported by NIH grant #100845 to G.M.W. F.T. was supported in part by the Institut Pasteur and a fellowship from the Association pour la Recherche sur le Cancer.

Received: October 26, 2005
Revised: February 27, 2006
Accepted: March 13, 2006
Published: April 10, 2006

References

Baptiste, N., Friedlander, P., Chen, X., and Prives, C. (2002). The proline-rich domain of p53 is required for cooperation with anti-neoplastic agents to promote apoptosis of tumor cells. Oncogene *21*, 9–21.

Berger, M., Vogt Sionov, R., Levine, A.J., and Haupt, Y. (2001). A role for the polyproline domain of p53 in its regulation by Mdm2. J. Biol. Chem. *276*, 3785–3790.

Bond, G.L., Hu, W., Bond, E.E., Robins, H., Lutzker, S.G., Arva, N.C., Bargonetti, J., Bartel, F., Taubert, H., Wuerl, P., et al. (2004). A single nucleotide polymorphism in the MDM2 promoter attenuates the p53 tumor suppressor pathway and accelerates tumor formation in humans. Cell *119*, 591–602.

Bottger, V., Bottger, A., Garcia-Echeverria, C., Ramos, Y.F., van der Eb, A.J., Jochemsen, A.G., and Lane, D.P. (1999). Comparative study of the p53-mdm2 and p53-MDMX interfaces. Oncogene *18*, 189–199.

Brooks, C.L., and Gu, W. (2004). Dynamics in the p53-Mdm2 ubiquitination pathway. Cell Cycle *3*, 895–899.

Chao, C., Hergenhahn, M., Kaeser, M.D., Wu, Z., Saito, S., Iggo, R., Hollstein, M., Appella, E., and Xu, Y. (2003). Cell type- and promoter-specific roles of Ser18 phosphorylation in regulating p53 responses. J. Biol. Chem. *278*, 41028–41033.

Chavez-Reyes, A., Parant, J.M., Amelse, L.L., de Oca Luna, R.M., Korsmeyer, S.J., and Lozano, G. (2003). Switching mechanisms of cell death in mdm2- and mdm4-null mice by deletion of p53 downstream targets. Cancer Res. *63*, 8664–8669.

Chen, L., Gilkes, D.M., Pan, Y., Lane, W.S., and Chen, J. (2005). ATM and Chk2-dependent phosphorylation of MDMX contribute to p53 activation after DNA damage. EMBO J. *24*, 3411–3422.

Chipuk, J.E., Kuwana, T., Bouchier-Hayes, L., Droin, N.M., Newmeyer, D.D., Schuler, M., and Green, D.R. (2004). Direct activation of Bax by p53 mediates mitochondrial membrane permeabilization and apoptosis. Science *303*, 1010–1014.

Danovi, D., Meulmeester, E., Pasini, D., Migliorini, D., Capra, M., Frenk, R., de Graaf, P., Francoz, S., Gasparini, P., Gobbi, A., et al. (2004). Amplification of Mdmx (or Mdm4) directly contributes to tumor formation by inhibiting p53 tumor suppressor activity. Mol. Cell. Biol. *24*, 5835–5843.

Donehower, L.A., Harvey, M., Slagle, B.L., McArthur, M.J., Montgomery, C.A., Jr., Butel, J.S., and Bradley, A. (1992). Mice deficient for p53 are developmentally normal but susceptible to spontaneous tumours. Nature *356*, 215–221.

Dornan, D., Shimizu, H., Burch, L., Smith, A.J., and Hupp, T.R. (2003). The proline repeat domain of p53 binds directly to the transcriptional coactivator p300 and allosterically controls DNA-dependent acetylation of p53. Mol. Cell. Biol. *23*, 8846–8861.

Dumaz, N., Milne, D.M., Jardine, L.J., and Meek, D.W. (2001). Critical roles for the serine 20, but not the serine 15, phosphorylation site and for the polyproline domain in regulating p53 turnover. Biochem. J. *359*, 459–464.

Edwards, S.J., Hananeia, L., Eccles, M.R., Zhang, Y.F., and Braithwaite, A.W. (2003). The proline-rich region of mouse p53 influences transactivation and apoptosis but is largely dispensable for these functions. Oncogene *22*, 4517–4523.

Finch, R.A., Donoviel, D.B., Potter, D., Shi, M., Fan, A., Freed, D.D., Wang, C.Y., Zambrowicz, B.P., Ramirez-Solis, R., Sands, A.T., and Zhang, N. (2002). mdmx is a negative regulator of p53 activity in vivo. Cancer Res. *62*, 3221–3225.

Francoz, S., Froment, P., Bogaerts, S., De Clercq, S., Maetens, M., Doumont, G., Bellefroid, E., and Marine, J.C. (2006). Mdm4 and Mdm2 cooperate to inhibit p53 activity in proliferating and quiescent cells in vivo. Proc. Natl. Acad. Sci. USA *103*, 3232–3237.

Gu, J., Kawai, H., Nie, L., Kitao, H., Wiederschain, D., Jochemsen, A.G., Parant, J., Lozano, G., and Yuan, Z.M. (2002). Mutual dependence of MDM2 and MDMX in their functional inactivation of p53. J. Biol. Chem. *277*, 19251–19254.

Hengstermann, A., Whitaker, N.J., Zimmer, D., Zentgraf, H., and Scheffner, M. (1998). Characterization of sequence elements involved in p53 stability regulation reveals cell type dependence for p53 degradation. Oncogene *17*, 2933–2941.

Johnson, T.M., and Attardi, L.D. (2005). p53QS: an old mutant teaches us new tricks. Cell Cycle *4*, 731–734.

Jones, S.N., Roe, A.E., Donehower, L.A., and Bradley, A. (1995). Rescue of embryonic lethality in Mdm2-deficient mice by absence of p53. Nature *378*, 206–208.

Kawai, H., Wiederschain, D., Kitao, H., Stuart, J., Tsai, K.K., and Yuan, Z.M. (2003). DNA damage-induced MDMX degradation is mediated by MDM2. J. Biol. Chem. *278*, 45946–45953.

Krummel, K.A., Lee, C.J., Toledo, F., and Wahl, G.M. (2005). The C-terminal lysines fine-tune p53 stress responses in a mouse model, but are not required for stability control or transactivation. Proc. Natl. Acad. Sci. USA *102*, 10188–10193.

Lev Bar-Or, R., Maya, R., Segel, L.A., Alon, U., Levine, A.J., and Oren, M. (2000). Generation of oscillations by the p53-Mdm2 feedback loop: a theoretical and experimental study. Proc. Natl. Acad. Sci. USA *97*, 11250–11255.

Linares, L.K., Hengstermann, A., Ciechanover, A., Muller, S., and Scheffner, M. (2003). HdmX stimulates Hdm2-mediated ubiquitination and degradation of p53. Proc. Natl. Acad. Sci. USA *100*, 12009–12014.

Liu, G., Parant, J.M., Lang, G., Chau, P., Chavez-Reyes, A., El-Naggar, A.K., Multani, A., Chang, S., and Lozano, G. (2004). Chromosome stability, in the absence of apoptosis, is critical for suppression of tumorigenesis in Trp53 mutant mice. Nat. Genet. *36*, 63–68.

Lowe, S.W., Ruley, H.E., Jacks, T., and Housman, D.E. (1993). p53-dependent apoptosis modulates the cytotoxicity of anticancer agents. Cell *74*, 957–967.

Mantovani, F., Gostissa, M., Collavin, L., and Del Sal, G. (2004). KeePin' the p53 family in good shape. Cell Cycle *3*, 905–911.

Marine, J.C., and Jochemsen, A.G. (2005). Mdmx as an essential regulator of p53 activity. Biochem. Biophys. Res. Commun. *331*, 750–760.

McCoy, M.A., Gesell, J.J., Senior, M.M., and Wyss, D.F. (2003). Flexible lid to the p53-binding domain of human Mdm2: implications for p53 regulation. Proc. Natl. Acad. Sci. USA *100*, 1645–1648.

Meulmeester, E., Maurice, M.M., Boutell, C., Teunisse, A.F., Ovaa, H., Abraham, T.E., Dirks, R.W., and Jochemsen, A.G. (2005). Loss of HAUSP-mediated deubiquitination contributes to DNA damage-induced destabilization of Hdmx and Hdm2. Mol. Cell *18*, 565–576.

Migliorini, D., Denchi, E.L., Danovi, D., Jochemsen, A., Capillo, M., Gobbi, A., Helin, K., Pelicci, P.G., and Marine, J.C. (2002). Mdm4 (Mdmx) regulates p53-induced growth arrest and neuronal cell death during early embryonic mouse development. Mol. Cell. Biol. *22*, 5527–5538.

Miller, F.D., Pozniak, C.D., and Walsh, G.S. (2000). Neuronal life and death: an essential role for the p53 family. Cell Death Differ. *7*, 880–888.

Montes de Oca Luna, R., Wagner, D.S., and Lozano, G. (1995). Rescue of early embryonic lethality in mdm2-deficient mice by deletion of p53. Nature *378*, 203–206.

Nister, M., Tang, M., Zhang, X.Q., Yin, C., Beeche, M., Hu, X., Enblad, G., van Dyke, T., and Wahl, G.M. (2005). p53 must be competent for transcriptional regulation to suppress tumor formation. Oncogene *24*, 3563–3573.

O'Gorman, S., Dagenais, N.A., Qian, M., and Marchuk, Y. (1997). Protamine-Cre recombinase transgenes efficiently recombine target sequences in the male germ line of mice, but not in embryonic stem cells. Proc. Natl. Acad. Sci. USA *94*, 14602–14607.

Okamoto, K., Kashima, K., Pereg, Y., Ishida, M., Yamazaki, S., Nota, A., Teunisse, A., Migliorini, D., Kitabayashi, I., Marine, J.C., et al. (2005). DNA damage-induced phosphorylation of MdmX at serine 367 activates p53 by targeting MdmX for Mdm2-dependent degradation. Mol. Cell. Biol. *25*, 9608–9620.

Parant, J., Chavez-Reyes, A., Little, N.A., Yan, W., Reinke, V., Jochemsen, A.G., and Lozano, G. (2001). Rescue of embryonic lethality in Mdm4-null mice by loss of Trp53 suggests a nonoverlapping pathway with MDM2 to regulate p53. Nat. Genet. *29*, 92–95.

Pereg, Y., Shkedy, D., de Graaf, P., Meulmeester, E., Edelson-Averbukh, M., Salek, M., Biton, S., Teunisse, A.F., Lehmann, W.D., Jochemsen, A.G., and Shiloh, Y. (2005). Phosphorylation of Hdmx mediates its Hdm2- and ATM-dependent degradation in response to DNA damage. Proc. Natl. Acad. Sci. USA *102*, 5056–5061.

Ren, J., Shi, M., Liu, R., Yang, Q.H., Johnson, T., Skarnes, W.C., and Du, C. (2005). The Birc6 (Bruce) gene regulates p53 and the mitochondrial pathway of apoptosis and is essential for mouse embryonic development. Proc. Natl. Acad. Sci. USA *102*, 565–570.

Roth, J., Koch, P., Contente, A., and Dobbelstein, M. (2000). Tumor-derived mutations within the DNA-binding domain of p53 that phenotypically resemble the deletion of the proline-rich domain. Oncogene *19*, 1834–1842.

Sakamuro, D., Sabbatini, P., White, E., and Prendergast, G.C. (1997). The polyproline region of p53 is required to activate apoptosis but not growth arrest. Oncogene *15*, 887–898.

Steinman, H.A., Sluss, H.K., Sands, A.T., Pihan, G., and Jones, S.N. (2004). Absence of p21 partially rescues Mdm4 loss and uncovers an antiproliferative effect of Mdm4 on cell growth. Oncogene *23*, 303–306.

Steinman, H.A., Hoover, K.M., Keeler, M.L., Sands, A.T., and Jones, S.N. (2005). Rescue of Mdm4-deficient mice by Mdm2 reveals functional overlap of Mdm2 and Mdm4 in development. Oncogene *24*, 7935–7940.

Stommel, J.M., and Wahl, G.M. (2004). Accelerated MDM2 auto-degradation induced by DNA-damage kinases is required for p53 activation. EMBO J. *23*, 1547–1556.

Sui, G., Affar el, B., Shi, Y., Brignone, C., Wall, N.R., Yin, P., Donohoe, M., Luke, M.P., Calvo, D., and Grossman, S.R. (2004). Yin Yang 1 is a negative regulator of p53. Cell *117*, 859–872.

Vassilev, L.T., Vu, B.T., Graves, B., Carvajal, D., Podlaski, F., Filipovic, Z., Kong, N., Kammlott, U., Lukacs, C., Klein, C., et al. (2004). In vivo activation of the p53 pathway by small-molecule antagonists of MDM2. Science *303*, 844–848.

Venot, C., Maratrat, M., Dureuil, C., Conseiller, E., Bracco, L., and Debussche, L. (1998). The requirement for the p53 proline-rich functional domain for mediation of apoptosis is correlated with specific PIG3 gene transactivation and with transcriptional repression. EMBO J. *17*, 4668–4679.

Vousden, K.H., and Lu, X. (2002). Live or let die: the cell's response to p53. Nat. Rev. Cancer *2*, 594–604.

Wahl, G.M., Stommel, J.M., Krummel, K.A., and Wade, M.A. (2005). Gatekeepers of the guardian: p53 regulation by post-translational modification, mdm2 and mdmx. In 25 Years of p53 Research, K. Wiman and P. Hainault, eds. (Berlin: Springer), pp. 73–113.

Walker, K., and Levine, A. (1996). Identification of a novel p53 functional domain that is necessary for efficient growth suppression. Proc. Natl. Acad. Sci. USA *93*, 15335–15340.

Xiong, S., Van Pelt, C.S., Elizondo-Fraire, A.C., Liu, G., and Lozano, G. (2006). Synergistic roles of Mdm2 and Mdm4 for p53 inhibition in central nervous system development. Proc. Natl. Acad. Sci. USA *103*, 3226–3231.

Zhu, J., Jiang, J., Zhou, W., Zhu, K., and Chen, X. (1999). Differential regulation of cellular target genes by p53 devoid of the PXXP motifs with impaired apoptotic activity. Oncogene *18*, 2149–2155.